



Published in final edited form as:

Arch Biochem Biophys. 2011 March 15; 507(2): 332–342. doi:10.1016/j.abb.2010.12.022.

DEUTERATION OF *ESCHERICHIA COLI* ENZYME I^{Ntr} ALTERS ITS STABILITY[§]

Grzegorz Piszczek¹, Jennifer C. Lee¹, Nico Tjandra¹, Chang-Ro Lee², Yeong-Jae Seok², Rodney L. Levine¹, and Alan Peterkofsky^{1,*}

¹The National Heart, Lung and Blood Institute, Bethesda, MD 20892, USA

²Department of Biophysics and Chemical Biology, Seoul National University, Seoul 151-742

Abstract

Enzyme I^{Ntr} is the first protein in the nitrogen phosphotransferase pathway. Using an array of biochemical and biophysical tools, we characterized the protein, compared its properties to that of EI of the carbohydrate PTS and, in addition, examined the effect of substitution of all nonexchangeable protons by deuterium (perdeuteration) on the properties of EI^{Ntr}. Notably, we find that the catalytic function (autophosphorylation and phosphotransfer to NPr) remains unperturbed while its stability is modulated by deuteration. In particular, the deuterated form exhibits a reduction of approximately 4 °C in thermal stability, enhanced oligomerization propensity, as well as increased sensitivity to proteolysis *in vitro*. We investigated tertiary, secondary, and local structural changes, both in the absence and presence of PEP, using near- and far-UV circular dichroism and Trp fluorescence spectroscopy. Our data demonstrate that the aromatic residues are particularly sensitive probes for detecting effects of deuteration with an enhanced quantum yield upon PEP binding and apparent decreases in tertiary contacts for Tyr and Trp side chains. Trp mutagenesis studies showed that the region around Trp522 responds to binding of both PEP and NPr. The significance of these results in the context of structural analysis of EI^{Ntr} are evaluated.

Keywords

phosphotransferase system; deuteration; conformation; protein structure

The *Escherichia coli* phosphoenolpyruvate:carbohydrate phosphotransferase system (PTS) is the major system for carbohydrate transport in that organism [1]. It consists of two proteins, EI and HPr, which function by sequential phosphorylation from PEP to EI, then to HPr; phospho-HPr can phosphorylate a collection of sugar-specific transporters which then go on to effect the uptake of a variety of sugar substrates. In addition to its role in sugar transport, the PTS functions in other regulatory capacities, primarily *via* control of the state of phosphorylation of the ~17 kDa protein IIA^{Glc}. The structures of numerous PTS proteins have been elucidated using X-ray crystallography and NMR spectroscopy [1]. Of note, the

[§]This work is dedicated to the memory of Ann Ginsburg who died on February 25, 2008. She was an important long-term collaborator on joint studies of proteins of the carbohydrate PTS and served as an Associate Editor of Archives of Biochemistry and Biophysics.

*address correspondence to this author at: National Institutes of Health, Building 50, Room 2316, Bethesda, MD, 20892-3017; peterkofsky@nih.gov; telephone 301-496-2408; FAX 301-402-1519.

Publisher's Disclaimer: This is a PDF file of an unedited manuscript that has been accepted for publication. As a service to our customers we are providing this early version of the manuscript. The manuscript will undergo copyediting, typesetting, and review of the resulting proof before it is published in its final citable form. Please note that during the production process errors may be discovered which could affect the content, and all legal disclaimers that apply to the journal pertain.

structure of the EI component, a protein with 575 amino acid residues, has been deduced by X-ray crystallography [2] and it has been proposed that the catalytic activity of this protein involves a swiveling domain mechanism similar to that demonstrated for pyruvate phosphate dikinase [3].

The PTS^{Ntr}, a system paralogous to that of the carbohydrate PTS, is comprised of the proteins EI^{Ntr}, NPr and IIA^{Ntr} (homologous to EI, HPr and IIA of the carbohydrate PTS). A major role for IIA^{Ntr} in regulation has been demonstrated. In this regard, it has been shown that the dephosphorylated form of IIA^{Ntr} binds to and inhibits the activity of TrkA, one of the potassium transporter activities of *E. coli* [4]. It was demonstrated that dephospho-IIA^{Ntr} also interacts with and stimulates the sensor kinase KdpD [5]. This ultimately leads to regulation of the expression of the high-affinity K⁺ transporter KdpFABC.

While the structures of NPr [6] and IIA^{Ntr} [7] have been solved, that of EI^{Ntr} is unknown. Although the primary structures of EI and EI^{Ntr} are homologous, there are clear differences in their activities. In a sugar phosphorylation assay, the turnover number for EI^{Ntr} is about 0.1% that for EI, which probably explains why EI is absolutely required for sugar phosphorylation *in vivo* [8]. Further, there is essentially absolute specificity of EI^{Ntr} for NPr suggesting that specific residues of EI^{Ntr} control the interaction and phosphoryl transfer between the proteins [8]. It was therefore of fundamental interest to define the three-dimensional structure of EI^{Ntr}; until this time, all attempts to produce crystals of EI^{Ntr} with suitable diffraction properties have been unsuccessful (Hertzberg and Peterkofsky, unpublished data). Consequently, alternative strategies (biophysical and NMR studies) to characterize EI^{Ntr} were undertaken. In preparation for preliminary NMR studies, we prepared perdeuterated protein and noted changes in properties. We therefore carried out companion biophysical, enzymatic and stability studies on both the hydrogenated and perdeuterated forms of EI^{Ntr} to both characterize EI^{Ntr} and evaluate the suitability of the perdeuterated EI^{Ntr} for structural analysis. The work described here documents similarities and differences in the two forms of the protein.

Materials and Methods

Materials

NPr, deficient in the terminal 8 amino acids (NPr 1–85), was prepared as described [6]. ³²P-PEP was prepared as described [9].

Cloning and expression of EI^{Ntr}—Full-length EI^{Ntr} is a protein of 748 residues. This protein is homologous to the 575 residue EI of the carbon PTS but, in addition, encodes a GAF domain at its N-terminus [10]. Initial experiments indicated that the expressed full-length protein tended to aggregate. Consequently, a truncated version of EI^{Ntr} that was homologous to EI was engineered in which the first 169 residues, encoding the unique GAF domain, were eliminated. This is subsequently referred to as EI^{Ntr}. Details of the cloning are in Supplementary Data. The expression vector encodes residues 170–748 of EI^{Ntr} preceded by MGSS(H)₆SSGLVPRGSHM (see Fig. 1). This amino-terminal His-tag sequence allows for rapid purification by IMAC. Details of protein expression and purification are in Supplementary Data. The yield of protein was about 10 mg (H)/liter and 5 mg (D)/500 ml. Analysis by mass spectrometry of the active-site peptide, produced by tryptic hydrolysis, indicated that both purified proteins were approximately 80% phosphorylated. The isolated proteins were demonstrated to be active in phosphoryl transfer from PEP/Mg to purified NPr.

Preparation of dephosphorylated H-EI^{Ntr} and D-EI^{Ntr} was accomplished by incubation with pyruvate (the back reaction). To one ml samples of each form of the protein, MgCl₂ and

sodium pyruvate were added to a final concentration of 10 mM and the solutions were incubated for 1 h at 37 °C. The samples were then processed on a Superose 6 HR 10/30 (GE Healthcare) column equilibrated with the Tris, glycerol, NaCl, EDTA, β -mercaptoethanol buffer described above. Fractions (1 ml) were screened by SDS-PAGE and fractions containing the protein were pooled, then concentrated using Amicon Ultra (Ultracel-3K) centrifugal filters (Millipore). Analysis by mass spectroscopy verified that the protein was completely dephosphorylated (calculated = 66711.8; observed = 66710.7).

A clone encoding EI^{Ntr} with the active-site His changed to Ala (H356A) was constructed (see Fig. 1). The details are described in Supplementary Data. The protein was expressed in both H₂O and D₂O media and purified by the same procedure as described above for the enzyme without the mutation. The yield of purified protein was 25 mg (H) from a 1 liter culture and 7.5 mg (D) from a 500 ml culture. The expressed protein from the H₂O culture was analyzed by mass spectroscopy and shown to contain a fraction with a mass of 66,646.7 Da, corresponding to the mutated protein devoid of the N-terminal Met (calculated = 66,645.7; see Fig. 1).

The purified proteins were analyzed to determine the degree of deuteration (Table I). Since the carbon source (glucose) was not deuterated, the expected level of deuteration was in the vicinity of 90% rather than 100% [11]. For the wild-type form of EI^{Ntr}, the predominant form isolated was both phosphorylated at the active site and gluconoylated at the site of the His tag [12] (calculated mass of the H form = 66,969.8)(Table I). The measured mass of that form corresponded accurately to the calculation. The measured mass of the deuterated form was 70,223.8 which corresponds to 89% deuteration. This matches very well to the expected level of deuteration under the culture conditions used.

The experiments for testing the effect of deuteration on autophosphorylation activity required the use of dephosphorylated protein. Dephosphorylation was accomplished by pyruvate treatment. Mass analysis showed that a byproduct of this treatment is that the protein can form an adduct (Schiff base) with pyruvate that increases the mass by 70 units (data not shown). The species analyzed was that of the gluconoylated form (calculated mass=66,889.8). The level of deuteration, as expected, remains at 89% (Table I).

For the form of EI^{Ntr} mutated at the active site (EI^{Ntr}(H356A)), the major form of the protein observed was gluconoylated (mass=66,823.7) and the level of deuteration was 88% (Table I).

We explored the possibility that some component of the measured deuteration might be due to exchangeable deuterium and that the level of nonexchangeable deuteration was less than approximately 90%. In order to evaluate this possibility, the level of deuteration of a tryptic peptide (the active site peptide) was measured (Table I); since such a peptide would be completely unfolded, all exchangeable deuterium would be replaced by hydrogen. The analysis of this peptide showed that the level of deuteration matched that seen in the protein preparations. Thus, all of the observed deuteration is in stable nonexchangeable positions.

Mass spectroscopic analysis also detected a truncated form(s) in both the H- and D-preparations of the wild-type and mutant forms of EI^{Ntr}. There is a pair of arginine residues occupying the 11th and 12th positions from the C-terminal end of the protein (see Fig. 1). The calculated masses of protein products truncated at the C-terminal side of either of these arginine residues is close to the observed masses of the truncated forms of the proteins. Thus, it appears that EI^{Ntr} becomes partially truncated by a trypsin-like activity *in vivo*. The extent of truncation is slightly greater for the deuterated species compared to the hydrogenated forms, a clue to the observed greater susceptibility of the deuterated protein to proteolysis *in vitro*.

Tryptophan mutants of EI^{Ntr}—For mapping studies of fluorescence effects in EI^{Ntr}, the 4 Trp residues of EI^{Ntr}(H356A) were mutated to Phe by changing the Trp codons of W186, W270, W319 and W522 (Figure 1) to UUU, corresponding to Phe. The pET28a-EI^{Ntr}(H356A) DNA was used as the template for QuikChange (Stratagene) mutagenesis. For unexplained reasons, we were unable to isolate a clone harboring the W270F mutation. The other 3 mutants were verified by mass analysis of the purified EI^{Ntr} proteins, which were purified by the same methods as described for the native protein.

Arginase—Purified human arginase I was a gift from Dr. David Christianson [13]. Paste from cells expressing perdeuterated human arginase I was kindly provided by Kate Thorn from the Christianson laboratory; the perdeuterated protein was prepared according to the published procedure [13].

Synuclein—*E. coli* harboring a pET41a hybrid plasmid expressing full-length α -synuclein was a kind gift from Dr. Nelson Cole [14]. Expression and purification of this protein are described in Supplementary Data. In the course of examination of the fractionation properties of α -synuclein on a reverse phase column, the observation was made that the perdeuterated form of the protein eluted earlier than did the hydrogenated form (Fig. 1 of Supplementary Data). This is evidence that deuterated proteins are less hydrophobic than hydrogenated forms of the same protein.

Methods

Mass spectrometry—HPLC-mass spectrometric analysis of tryptic peptides: The assay for phosphotransfer from EI^{Ntr} to NPR depended on HPLC separation of EI^{Ntr} tryptic peptides followed by mass spectrometric analysis. An Agilent model 1100 HPLC with a Zorbax 300SB-C18, 1.0 × 50 mm 3.5 micron (Agilent Technologies) column flowing at 20 μ l/min was used. The initial solvent was 0.05% trifluoroacetic acid with gradient elution by acetonitrile/0.05% trifluoroacetic acid (TFA) increasing at 2%/min from 0 to 70%. The effluent from the spectrophotometric detector was mixed in a tee (Upchurch M540) with 20 μ l/min acetic acid pumped by another model 1100 pump, and the mixture was introduced into a model G1969A mass spectrometer (Agilent)[15] with time of flight detector. The mass range from 145 to 2000 amu was scanned at 10,000 transients/scan. Voltages were: capillary, 5000 V; fragmentor, 235 V; skimmer, 60 V; and octopole RF, 250 V. The ion source gas temperature was 350 °C, drying gas flow was 10 l/min, and nebulizer gas pressure was 10 psig. Reference mass correction utilized an infused standard of 922 amu and metal-acetic acid clusters from 173 to 537 amu generated in the electrospray [16]. For direct infusion analysis of intact proteins without a column, the only change in the HPLC-MS method was that the HPLC pumped 0.05% TFA without a gradient.

Differential scanning calorimetry (DSC)—DSC measurements were carried out using a VP-DSC calorimeter (MicroCal) as previously described [17]. The scan rate was 30 °C/h. The data was corrected for instrument baselines. Data analysis was performed using Origin software (MicroCal). Excess heat capacity (C_p) was expressed in kcal K⁻¹ (mol monomer)⁻¹, where 1000 cal = 4.184 J.

Isothermal Titration Calorimetry—Binding studies were performed at 20 °C in 20 mM sodium phosphate, pH 8, 100 mM NaCl, 5 mM MgCl₂ in a VP-ITC titration calorimeter (MicroCal, LLC, Northampton, MA, U.S.A.) with a reaction cell volume of 1.4 ml. Typically, about 15 μ M EI^{Ntr} in the reaction cell was titrated with a stock solution of about 400 μ M NPR contained in a 250 μ l syringe. Consecutive injections corresponded to ~8–9% of the total [EI^{Ntr}] in the ITC cell at 6- to 8-minute intervals, while stirring the protein solution at 260 rpm constant speed. The heat of dilution of NPR was determined by

averaging the final 5–10 injections. Titration curves were analyzed with the Origin program provided by MicroCal, LLC, using one or two classes of binding sites to fit the curves.

Fluorescence Measurements—Fluorescence measurements (excitation at 295 nm and emission at 340 nm) were made using a QM-6SE (PTI, London, Ontario) spectrofluorometer. Reaction mixtures (1 ml volume) were maintained at 37 °C under constant stirring. Sample temperature was controlled by a Peltier sample holder. All spectral measurements were performed with Glan polarizers at magic angle conditions and excitation wavelength 295 nm for the intrinsic tryptophan residue fluorescence measurements. Aliquots of concentrated stock solutions of either PEP or NPr were added as indicated in the respective figures and the fluorescence change was recorded. The changes in fluorescence were corrected for dilution resulting from addition of NPr or PEP.

Light scattering measurements—A DAWN EOS (Wyatt Technology, Santa Barbara, CA) equipped with a flow cell and a 30 mW linearly polarized GaAs laser of wavelength 690 nm was used with measurements in the in-line flow mode. An HPLC pump was used to deliver filtered solvent through a Phenomenex BioSef-SEC-S2000 gel filtration column. Protein samples were injected in a volume of 100 μ l. Both the light scattering unit and the refractometer (Waters 2419 refractive index detector) were calibrated as per the manufacturer's instructions. A value of 0.185 ml/g was assumed for the dn/dc of the protein. Light scattering data were from 11 detectors ranging from 50.0° to 134° (detectors 6 through 16). The detector responses were normalized by measuring the signal from monomeric bovine serum albumin. The flow rate was maintained at 0.5 ml/min. The traces from the DAWN EOS and refractometer were analyzed with ASTRA-V software to obtain the weight-average molecular weight (Red lines).

Circular dichroism—Circular dichroism measurements were carried out as described [18].

Autophosphorylation of EI^{Ntr}—For the kinetic experiments, the stock solutions of both EI^{Ntr} preparations contained 21.4 pmoles of autophosphorylatable protein (dephosphorylated EI^{Ntr}) in each 15 μ l stop-quench shot. The EI^{Ntr} solutions contained 10 mM Tris-Cl, pH 8, 10% glycerol, 100 mM NaCl, 1 mM EDTA, and 2 mM β -mercaptoethanol. The ³²P-PEP solution (see Materials) contained 75 mM Tris-Cl, pH 8, 15 mM MgCl₂, 15 mM β -mercaptoethanol and 300 μ M PEP (specific activity ~400 cpm/pmole). The quench solution was 4 \times SDS Laemmli sample buffer, 30 mM EDTA. Quench-flow experiments were carried out in a KinTek Corp. Model RQF-3 Quench-Flow instrument at 37 °C where one syringe was loaded with EI^{Ntr} solution, another with ³²P-PEP solution and the third with quench solution. Each shot contained 15 μ l of the EI^{Ntr} and PEP solutions, delivered by a Kds Pico Plus syringe pump. The volume of each quenched sample was determined; 60 μ l aliquots were deposited onto 10-well 4–20% Tris-glycine gradient gels (Invitrogen). Electrophoresis was carried out for 1.5 hours at 130 volts. The gels were stained for 40 min with Coomassie Blue R250, then destained for 30 min. The stained bands were excised from the gels and counted with 5 ml of scintillation fluid. From the cpm observed for the 60 μ l aliquot, the volume of the original quenched sample, the specific activity of the ³²P-PEP and the total pmoles EI^{Ntr} (21.4), the % of phosphorylation was calculated.

Phosphotransfer from P-EI^{Ntr} to NPr—Cocktails were prepared in a 200 μ l volume containing: Tris-Cl, pH 7.5, 60 mM; MgCl₂, 1.2 mM; KCl, 12 mM; EI^{Ntr} (H or D), 11.5 μ g. Aliquots (25 μ l) were dispensed into tubes and reactions were initiated by the addition of NPr 1–85 (5 μ l containing a 10-fold molar excess of NPr, 2.1 μ g). Incubations were at room temperature. At the indicated times, reactions were terminated by the addition of 30 μ l of

quench solution (5 M urea, 3 M KOH). After adding 300 μ l of H₂O and 300 μ l of 1 M Tris-Cl, pH 8, the samples were added to 100 μ l of washed Talon beads and incubated with shaking for 1 h at 4 °C. The beads were then washed 4 times with 0.5 ml aliquots of 25 mM Tris-Cl, pH 8, 200 mM NaCl. The washed beads were suspended in 40 μ l of 25 mM Tris-Cl, pH 8, 200 mM NaCl, 100 mM imidazole and 1 μ g trypsin was added. After incubation at room temperature for 1 h with periodic shaking, the Talon beads were centrifuged and a 25 μ l aliquot of the supernatant solution was transferred to a vial for analysis by mass spectrometry. The fraction of the active site peptide in the phosphorylated form is plotted against the incubation time.

Results and Discussion

1.1 Proteolysis of EI^{Ntr}

Analysis of the progress of tryptic hydrolysis of EI^{Ntr}(H356A) (see Fig. 1) by mass spectroscopy enabled a description of the pathway of degradation of the protein (see Fig. 2 of Supplementary Data). The initial attack on the His-tagged protein resulted in elimination of the major fraction of the His-tag (peptide with mass of 1767.84). Subsequently, the residual protein (mass of 64,894.9) was split into an N-terminal fragment (mass=39,794.4) and a C-terminal fragment (mass=25,118.5). Next, the C-terminal fragment was degraded to two fragments (masses of 12,688.9 and 12447.6). The N-terminal fragment was not further degraded during the time course of the experiment (90 min). The unambiguous identification of the location of the fragments within the EI^{Ntr} sequence (Fig. 2 of Supplementary Data) was possible because of the mass accuracy of the analyses.

A previous description of proteolysis by trypsin of EI [19,20] demonstrated the stable accumulation of the N-terminal portion of the protein (peptide 1–255, mass=27833). A local alignment of EI and EI^{Ntr} in the region corresponding to loop 3 [2] of EI (Fig. 3 of Supplementary Data) shows that the region around R523 of EI^{Ntr} is almost identical in the EI sequence, but the region around K255 of the EI sequence does not have a corresponding trypsin site in the EI^{Ntr} sequence. Consequently, it seems reasonable to propose that, for EI, the initial cleavage site is at R358 followed by cleavage at K255 resulting in the accumulation of EIN. In the case of EI^{Ntr}, the initial cleavage is at R523; since there is no trypsin site corresponding to K255 of EI, there is no further proteolysis in the N-terminal region of EI^{Ntr}. Therefore, EI and EI^{Ntr} have the similar property of having a stable N-terminal region; however, the two proteins differ in the precise region of the linker between the N-terminal and C-terminal domains that are susceptible to trypsin. This may point to one of the factors that determine the difference in specificity [8] of the two proteins.

Based on the mass analysis of the purified preparations of EI^{Ntr} (see Materials and Methods), we suspected that EI^{Ntr} in the deuterated form was more susceptible to *in vivo* proteolysis. Consequently, a kinetic comparison was made of H-EI^{Ntr} and D-EI^{Ntr} with respect to the sensitivity to limited proteolysis by trypsin (Fig. 2). In order to avoid the complication of analysis of a mixture of phospho- and dephosphopeptides, the inactive H356A mutant of EI^{Ntr} (see Fig. 1) was used for the study; this active site mutant is incapable of becoming phosphorylated. The kinetics of proteolysis were followed over a period of 90 min. SDS-PAGE analysis clearly shows that the rates of disappearance of the Coomassie Blue stained band corresponding to the intact protein (uppermost arrow in Panel A) are different for the two proteins (Panel A); D-EI^{Ntr} is degraded faster than is H-EI^{Ntr}. Inclusion of an excess of NPr (Panel B) in the proteolysis reaction does not protect EI^{Ntr} from proteolysis although the kinetics of scission, producing intermediate products (panels E through H) is somewhat influenced by the presence of NPr. This study provides further evidence that D-EI^{Ntr} has a less stable structure than H-EI^{Ntr}.

There is precedent for some perdeuterated proteins exhibiting less stability in proteolysis experiments. In 1965, Hattori et al [21] reported that phycocyanin with deuterated side-chains exhibited a destabilization resulting in an increased sensitivity to *in vitro* proteolysis. They argued that deuteration of nonexchangeable hydrogen positions decreases nonpolar side-chain interactions with an effect on the conformational integrity of proteins. This was the result of less crowding, leading to reduced hydrophobic interactions and, possibly, increased dynamics. They proposed that the initial step in tryptic hydrolysis required substrate denaturation necessary to overcome the steric hindrance to hydrolysis.

In another study, H- and D-forms of the 26 kDa homodimeric glutathione S-transferase were compared for susceptibility to proteolysis by chymotrypsin; the perdeuterated protein was hydrolyzed considerably faster than the hydrogenated form [11]. It was suggested that barriers to local unfolding, presumably a necessary requirement for proteolysis, are reduced in the deuterated protein. In summary, there are several precedents for the observation that perdeuteration of some proteins may be coupled to increased susceptibility to proteolysis.

1.2 Proteolysis of Human Arginase

We posed the question of whether a protein that has been shown to have an unchanged three dimensional structure upon perdeuteration would also show an increased susceptibility to proteolysis. Human arginase I, in complex with the substrate analog 2(S)-amino-6-borono-hexanoic acid (ABH) has been crystallized in both the unlabeled and perdeuterated forms [13]. The findings were that the structure of the arginase I-ABH complex was not changed by perdeuteration. We studied the sensitivity to tryptic hydrolysis of the two forms of arginase I. Initial studies of the proteolysis by trypsin indicated that both forms of the protein (a gift from Dr. David Christianson) were essentially completely resistant to hydrolysis. The protein has been shown to contain a binuclear manganese cluster [22] which plays an important role in stabilizing the structure [23]. Thus, the form of the protein which was crystallized was stabilized by both manganese as well as the substrate analog. However, when we tested the hydrogenated and perdeuterated forms of arginase for proteolysis by trypsin in the presence of 1 mM EDTA, which released manganese from the arginase, hydrolysis was observed (Fig. 4 of Supplementary Data). Similar to the case with EI^{Ntr}, the perdeuterated form of the protein exhibited a greater sensitivity to trypsin than did the normal form of arginase. As pointed out by Brockwell et al [11], the stability of stable proteins appears unaffected by deuteration. However, when arginase was somewhat destabilized, it was possible to detect a stability difference associated with deuteration. This is in keeping with the notion that hydrophobic interactions are diminished by deuteration.

1.3 Proteolysis of α -synuclein

The observation that perdeuteration of both EI^{Ntr} and arginase resulted in a destabilization as reflected in sensitivity to tryptic hydrolysis introduced the possibility that deuterated polypeptides were intrinsically better substrates for trypsin. To evaluate this possibility, we studied the properties of α -synuclein, which has been shown to be an intrinsically disordered protein in solution [24]. Full-length α -synuclein, expressed in *E. coli*, was prepared in both hydrogenated and perdeuterated forms (see Materials and Methods and Supplementary Data). The kinetic study of tryptic hydrolysis (Fig. 5 of Supplementary Data) showed that the rates are identical for the two forms of the protein. Thus, the possibility that a deuterated polypeptide is a better substrate for trypsin than a hydrogenated peptide was eliminated. Taken together, the experiments reported herein support the idea that perdeuteration of EI^{Ntr}, as well as arginase, results in structural destabilization as evidenced by a change in sensitivity to trypsin digestion. How the structural destabilization affects the three-dimensional structure of a protein is uncertain and may vary from protein to protein.

2.1 Thermal Unfolding of EI^{Ntr}

Previous studies by differential scanning calorimetry of EI unfolding described an unfolding pattern with a midpoint at about 52 °C [17]. A comparable study was performed with EI^{Ntr} and a similar unfolding profile was observed, suggesting that the stability of EI and EI^{Ntr} is similar (Fig. 3). Then, a comparison was made of the unfolding properties of perdeuterated EI^{Ntr} (D) and hydrogenated EI^{Ntr} (H). Thermal unfolding was studied through the range of 20 to 70 °C. The T_m values for unfolding were calculated by determination of the mid-points of the unfolding curves. For the fluorescence measurements (Panel A), D-EI^{Ntr} = 48.88 °C; H-EI^{Ntr} = 52.58 °C; deuterium dependent destabilization = 3.7 °C. For the calorimetry experiment (Panel B), the deuterium dependent destabilization was 3.4 °C. The effect of interaction of EI^{Ntr} with the ligand PEP on the stability of the two forms was also evaluated (panel A). D-P = 52.84 °C; stabilization due to PEP binding = 3.96 °C; H-P = 56.62 °C; stabilization due to PEP binding = 4.04 °C. Unfolding led to aggregation and precipitation of the proteins. Effects of perdeuteration of proteins on thermal stability have previously been noted. P450cam displays a reduction of 4–5 °C [25], glutathione-S-transferase [11] a reduction of 3.9 °C and phycocyanin [21] a reduction of 7 °C. Thus, similar to the case with sensitivity to proteolysis, the effect of perdeuteration on unfolding of some proteins is demonstrable with an effect on thermal stability.

3.1 Oligomerization State of EI^{Ntr}

Previous studies on EI of the carbohydrate PTS, a paralog of EI^{Ntr} [10], have demonstrated that the protein exhibits a monomer-dimer interconversion [17,26,27] and that dimerization is promoted by PEP. Early in purification attempts, differences in behavior of D-EI^{Ntr} were observed. A change of buffer from pH 8 to pH 7 frequently led to precipitation of D-EI^{Ntr}; long term storage of D-EI^{Ntr} (at 4 °C in 25 mM phosphate pH 8, 100 mM NaCl, 5 mM MgCl₂) also resulted in protein precipitation. In contrast, H-EI^{Ntr} was stable under these conditions. Consequently, we examined the oligomerization and aggregation properties of the two forms of EI^{Ntr} (Fig. 4). SDS-PAGE analysis (data not shown) indicated that both forms were essentially homogeneous under denaturing conditions. Gel filtration chromatography coupled to light scattering analysis of H-EI^{Ntr} (Fig. 4) showed that, at the protein concentration studied (about 20 times higher than the fluorescence study of Fig. 3A), H-EI^{Ntr} was mainly monomeric. When the gel filtration column was pre-equilibrated with 150 μM PEP, H-EI^{Ntr} became mainly dimeric (see red lines). It therefore appears that EI^{Ntr}, similar to EI, exhibits a monomer-dimer equilibrium which is shifted in the direction of dimer by PEP. Gel filtration analysis of D-EI^{Ntr} (Fig. 4 inset) demonstrated another significantly different property of that protein. It was obviously polydisperse with most of the protein eluting in the excluded volume. The conclusion from this study is that deuteration of EI^{Ntr} converts the protein from a relatively simple mixture of the monomeric and dimeric forms to a collection of many other species of oligomers. At this concentration and pH, addition of PEP to perdeuterated protein results in further aggregation and tendency to precipitate (data not shown).

Previous results dealing with the effect of perdeuteration on the associative properties of proteins showed a nonuniform picture. In the case of phycocyanin [21], deuteration resulted in a decreased tendency to associate into trimer and hexamer forms; in contrast, for glutathione-S-transferase [11], deuteration promoted dimer association. Consequently, it appears that the effect of perdeuteration on protein associative properties is unpredictable.

4.1 Secondary and Tertiary Structure of EI^{Ntr}

Possible changes in secondary and tertiary structure associated with deuteration of EI^{Ntr} were explored by circular dichroism (CD) spectroscopy. The typical far UV spectroscopy study showed little difference in the two forms of the protein indicating no major secondary

structure differences (Fig. 6 of Supplemental Data). In contrast, the near UV region (Fig. 5A) showed significant spectral differences suggesting changes to the tyrosine and tryptophan tertiary contacts, but not for the phenylalanine residues. The addition of PEP/Mg resulted in similar spectra (Fig. 5B) of the two forms of the protein. These data are consistent with the interpretation that the deuteration-dependent conformational change is due to changes in tertiary structure in the vicinity of one or more Trp and Tyr residues.

The previous work on P450cam [25] showed that deuteration led to a decrease in α -helix content and an increase in the unordered content; the authors nevertheless concluded that there was little effect on the structure and dynamics of the protein associated with deuteration.

5.1 Enzymatic Activities of EI^{Ntr}

5.1.1 Autophosphorylation—In light of the preceding observations concerning the decrease in stability of EI^{Ntr} associated with deuteration, it was of interest to explore the effect of deuteration on the catalytic activity of EI^{Ntr}. In contrast to the previous experiments which utilized the active site mutant of EI^{Ntr}, this experiment required the wild-type protein. The H and D forms of the wild-type protein were expressed and purified in the same manner as were the mutated forms. Since the proteins as isolated were mainly in the phospho-form (Table 1), they were subjected to a dephosphorylation procedure (see Materials and Methods). A kinetic study of the autophosphorylation by ³²P-PEP of the two forms was carried out using a stop-quench instrument (Fig. 6). Half-maximal autophosphorylation was achieved in approximately 120 msec. The results indicate no discernable difference in the kinetics of autophosphorylation of either form of the protein. The experiment was carried out at 37 °C, a temperature well below that at which unfolding takes place. Thus, although D-EI^{Ntr} is considerably less stable than H-EI^{Ntr}, catalytic activity for autophosphorylation appears to be unaffected. This is not surprising, since numerous studies [28,29] have indicated variable or no effects on catalytic activity associated with structural variation.

5.1.2 Phosphotransfer to NPr—In addition to the ability of EI^{Ntr} to be autophosphorylated by PEP, the phosphorylated protein is able to perform phosphotransfer to an active site histidine of NPr. Studies were carried out to evaluate the effect of deuteration on the capability of EI^{Ntr} to interact with and make a phosphotransfer to the acceptor, NPr.

As isolated, the purified preparations of both H- and D-EI^{Ntr} were at least 80% phosphorylated. These preparations were therefore suitable for *in vitro* experiments designed to measure the phosphotransfer to NPr (Fig. 7). The experiments used a 10-fold molar excess of NPr to drive the phosphotransfer reaction. Equilibrium was reached in approximately one min. It was noteworthy that the phosphotransfer reaction was very much slower than was the autophosphorylation reaction. Fifty percent completion of phosphotransfer was accomplished in approximately 20 sec. There was no detectable difference in the kinetics of the phosphotransfer reaction for the two forms of EI^{Ntr}.

Studies on the effect of deuteration on the catalytic properties of other proteins have shown a variety of differences, if any. Glutathione-S-transferase showed an increased rate of catalysis associated with deuteration [11]. In the case of ribulose biphosphate carboxylase [30], the activity of the deuterated form was only 28% that of the hydrogenated form and this functional defect was recovered by the addition of a chaperone. It was concluded that the deuterated enzyme has a defective folding relative to the hydrogenated form. In contrast, deuteration had no significant effect on the reactivity of cytochrome c peroxidase [31] or human arginase I [13].

6.1 Ligand Binding Studies

6.1.1 Interaction with PEP—Although the capability of EI^{Ntr} to be phosphorylated by PEP was unaffected by deuteration (Fig. 6), additional biophysical methods were used to study the interaction of EI^{Ntr} with PEP. In order to avoid the complication of PEP binding followed by phosphorylation, the active site mutant, H356A, which is capable of binding PEP but not phosphorylation, was again used.

EI^{Ntr}(H356A) contains 4 Trp residues, located at positions 186, 270, 319, and 522 (numbering as for the intact full-length protein; see Figure 1). Based on the likely similarity to the structure of EI of the carbohydrate PTS [2], Trp 270 was assumed to be in the NPr binding domain, Trp 186 and 319 in the His domain and Trp 522 in the PEP binding domain. Measurements of intrinsic Trp fluorescence have been widely used to monitor protein environment and conformational changes [32–34]. The emission properties are particularly sensitive to solvent polarity, microenvironment viscosity and molecular mobility.

At 0.5 μM , the two forms of the H356A protein exhibit similar fluorescence properties: $\lambda_{\text{max}} \sim 340 \text{ nm}$ and comparable quantum yields (see legend to Fig. 8). The effect of PEP concentration on Trp fluorescence of H- and D-EI^{Ntr} is shown in Fig. 8A. Upon sequential additions of PEP at 37 °C, Trp fluorescence intensities increase and reach saturation indicating complete binding. Interestingly, the titration data show a significant difference in the relative fluorescence increase in the two proteins upon PEP binding. The fluorescence change of D-EI^{Ntr} was approximately twice as great as that of H-EI^{Ntr}. Further, the dissociation constants (K_d) suggest that the binding affinities could be modulated by deuteration ($K_d(\text{H-EI}^{\text{Ntr}}) = 21 \mu\text{M}$ vs. $K_d(\text{D-EI}^{\text{Ntr}}) = 33 \mu\text{M}$). While the exact nature of the differences in quantum yield changes are generally difficult to determine directly, the greater fluorescence increase associated with PEP binding to D-EI^{Ntr} could reflect restriction of local mobility of one or more Trp residues in D-EI^{Ntr}. Alternatively, changes in local conformation can lead to differences in nonradiative relaxation (i.e., solvent exposure). Notably, the PEP effect on Trp fluorescence is highly dependent on the protein concentration (Fig. 8C); higher protein concentrations result in smaller PEP-dependent increases in fluorescence. It is likely that the Trp residues are sensitive to the monomer-dimer equilibrium and the apparent differences in PEP interaction may be attributable to changes in the oligomerization state.

Fluorescence quenching [35,36] has been widely used to determine the solvent exposure of fluorophores. It is assumed that quenching cannot occur when a fluorophore like Trp is located in the interior of a protein. Further insight into the relative conformational changes produced by interaction of PEP with either H- or D-EI^{Ntr} was gained by a study of quenching by iodide under various conditions (Fig. 9). The effect of iodide at concentrations up to 1 M on Trp fluorescence in the absence or presence of 2 mM PEP was measured. In both cases (absence or presence of PEP), the sensitivity of D-EI^{Ntr} to iodide quench was greater than for H-EI^{Ntr}. This indicates that at least one of the 4 Trp residues of EI^{Ntr} is more solvent exposed in D-EI^{Ntr} than in H-EI^{Ntr}, further evidence for a conformational difference associated with deuteration.

To gather some insight into the region of the protein involved with PEP binding, further fluorescence measurements were made using Trp to Phe mutants of EI^{Ntr} (Fig. 10A). As predicted above, the region in the vicinity of Trp522 appears to be important in the interaction with PEP. Mutations of Trp residues 186 or 319 have little effect on the fluorescence increase associated with PEP binding, while mutation of Trp522 essentially abolishes the PEP effect on fluorescence.

6.1.2 Interaction with NPr—A fluorescence experiment similar to that shown in Fig. 8A was carried out; in this case, the interaction of the two forms of EI^{Ntr} with NPr was studied. The results with NPr interaction (Fig. 8B) were different than those for interaction with PEP (Fig. 8A). The fluorescence increases for binding of NPr to either form of the protein were similar. It is noteworthy that the extent of fluorescence change due to addition of NPr was similar to that seen for the addition of PEP to H-EI^{Ntr} (Fig. 8A); the major difference in fluorescence changes was associated with the effect of PEP on D-EI^{Ntr}. The calculated K_d values for binding NPr to EI^{Ntr} forms did differ, however; for H-EI^{Ntr}, the K_d was 23 μM and for D-EI^{Ntr}, it was 43 μM . Thus, overall, it seemed that deuteration of EI^{Ntr} has a more profound effect on the interaction with PEP than for interaction with NPr.

Previous studies on EI of the carbohydrate PTS indicated that the isolated amino-terminal half of the protein (termed EIN) had the capability to bind the phosphoacceptor protein HPr [2,37]. We established that the comparable EIN construct of EI^{Ntr} was capable of binding NPr (unpublished studies of AP and E. Fodor). A study was therefore carried out (Fig. 10B) to determine the effect of NPr concentration on the fluorescence of the collection of Trp-Phe mutants that were used for the analogous experiments for PEP binding (Fig. 10A). Contrary to expectation, the Trp mutants in the amino-terminal half of the EI^{Ntr} demonstrated binding curves similar to the wild-type protein; only the W522F protein had lost the capability to show a Trp fluorescence response to NPr binding. These data suggest that the binding of NPr to the aminoterminal region of EI^{Ntr} promotes a conformational change in the loop 3 region encompassing W522. (see Figure 3 of Supporting Data). It is noteworthy that binding of HPr to EIN is not associated with a significant structural change in either protein [37]. Therefore, the absence of fluorescence effects on W186 or W319 attendant on NPr binding is not surprising. A further exploration of the characteristics of interaction of NPr with both H- (Fig. 11A) and D- (Fig. 11B) EI^{Ntr} was carried out by isothermal titration calorimetry. In both cases, the binding data fit reasonably well to a model for one binding site ($N \sim 0.7$) with a K_d of $\sim 7 \mu\text{M}$. Thus, little difference was detected between the two forms of EI^{Ntr} in either phosphotransfer activity or in calorimetric measurements of the binding of NPr.

7.1 Structural Considerations

Results in the literature concerning the effect of perdeuteration on structure do not present a uniform picture [38]. In some cases (human arginase I [13] and carbonic anhydrase [39]), it was concluded that deuteration has no discernible effect on structure. There are, however, reports detailing deuteration effects on structure. P450cam [25] showed a change in α -helix content associated with deuteration. Haloalkane dehalogenase [40] assumed similar conformations in both protein forms, but there were crucial differences in the active site. As yet, there have been no three-dimensional structures reported for EI^{Ntr} in either H- or D-forms. Since the protein is large and multi-domained, it is likely that a careful analysis of the structure of the two forms would reveal significant differences.

The collection of data presented here suggests that the locus of sensitivity to proteolysis (Fig. 2) and differential fluorescence effects upon ligand binding to perdeuterated EI^{Ntr} (Fig. 8) is in the flexible loop 3 region (Fig. 3 of Supporting Data) of the protein that links the two domains of the protein. This suggests the possibility that mutagenic manipulation of the amino acid sequence in this loop might minimize the difference in biophysical properties of the two protein forms. In such a case, structural data derived from NMR studies of EI^{Ntr} could be interpreted with more confidence.

Concluding Remarks

The biophysical and stability properties of EI^{Ntr} have been characterized. A collection of studies (proteolysis, unfolding, oligomerization, near UV CD, ligand binding measured by

Trp fluorescence) comparing the biophysical properties of the hydrogenated and perdeuterated forms of EI^{Ntr} provide evidence for structural and stability differences associated with perdeuteration. These differences may be explained by differences in molecular dynamics of the two forms of the protein. The data suggest potential complications in analyzing structural data using the perdeuterated form of this protein. The data further suggest that the loop 3 region of EI^{Ntr} is a favorable target for exploring structural changes that might stabilize the protein; such a form might provide less ambiguous structural information. It is worthy of note that the truncated EI^{Ntr} protein used in these studies lacks the normally occurring GAF domain and may differ in properties from the full-length protein; however, its structure should be quite analogous to its paralog, EI, and therefore serves as a good experimental model. The function of the GAF domain of EI^{Ntr} remains to be elucidated.

Supplementary Material

Refer to Web version on PubMed Central for supplementary material.

Acknowledgments

The authors acknowledge helpful discussions with Drs. Edward Korn (NIH), Osnat Herzberg and John Moult (Center for Advanced Research in Biotechnology), expert guidance in the use of the stop-quench instrument by Dr. James Sellers (NIH) as well as the excellent technical assistance of Nancy Wehr (NIH). We thank Dr. David Christianson (University of Pennsylvania) for gifts of hydrogenated and perdeuterated human arginase and Dr. Nelson Cole (NIH) for a gift of α -synuclein. YJS was supported by the National Research Foundation Grant (NRF 2010-0017384) funded by MEST, Korea.

This work was supported by the Intramural Research Program of the National Heart, Lung and Blood Institute.

Abbreviations

PTS	phosphotransferase system
EI	Enzyme I of the carbohydrate PTS
PTS^{Ntr}	nitrogen PTS
EI^{Ntr}	Enzyme I of the nitrogen PTS
H-EI^{Ntr}	the hydrogenated form of EI ^{Ntr}
D-EI^{Ntr}	the deuterated form of EI ^{Ntr}
perdeuterated protein	protein in which nonexchangeable, carbon-bound protons are replaced by deuterium
PEP	phosphoenolpyruvate
GAF domains	small-molecule-binding domains that recognize cGMP-binding cyclic nucleotide phosphodiesterases, adenyl cyclases, and the transcription factor FhlA
TROSY	transverse relaxation optimized spectroscopy
amu	atomic mass unit
IMAC	immobilized metal affinity chromatography

Reference List

- [1]. Deutscher J, Francke C, Postma PW. *Microbiology and Molecular Biology Revs.* 2006; 70:939–1031.

- [2]. Teplyakov A, Lim K, Zhu P-P, Kapadia G, Chen CC, Schwartz J, Howard A, Reddy P, Peterkofsky A, Herzberg O. Proc. Natl. Acad. Sci. USA. 2006; 103:16218–16223. [PubMed: 17053069]
- [3]. Herzberg O, Chen CC, Kapadia G, McGuire M, Carroll LJ, Noh SJ, Dunaway-Mariano D. Proc. Natl. Acad. Sci. , USA. 1996; 93:2652–2657. [PubMed: 8610096]
- [4]. Lee C-R, Cho S-H, Yoon M-J, Peterkofsky A, Seok Y-J. Proc. Natl. Acad. Sci. USA. 2007; 104:4124–4129. [PubMed: 17289841]
- [5]. Lüttmann D, Heermann R, Zimmer B, Hillmann A, Rampp IS, Jung K, Görke B. Mol. Microbiol. 2009; 72:978–994. [PubMed: 19400808]
- [6]. Li X, Peterkofsky A, Wang G. Amino. Acids. 2008; 35:531–539. [PubMed: 18421563]
- [7]. Wang G, Peterkofsky A, Keifer PA, Li X. Protein Sci. 2005; 14:1082–1090. [PubMed: 15741344]
- [8]. Rabus R, Reizer J, Paulsen I, Saier MH Jr. J. Biol. Chem. 1999; 274:26185–26191. [PubMed: 10473571]
- [9]. Roossien FF, Brink J, Robillard GT. Biochim. Biophys. Acta. 1983; 760:185–187. [PubMed: 6615882]
- [10]. Peterkofsky A, Wang G, Seok Y-J. Arch. Biochem. Biophys. 2006; 453:101–107. [PubMed: 17022110]
- [11]. Brockwell D, Yu L, Cooper S, McClelland S, Cooper A, Attwood D, Gaskell SJ. J. Barber, Protein Sci. 2001:572–580.
- [12]. Geoghegan KF, Dixon HB, Rosner PJ, Hoth LR, Lanzetti AJ, Borzilleri KA, Marr ES, Pezzullo LH, Martin LB, LeMotte PK, McColl AS, Kamath AV, Stroh JG. Anal. Biochem. 1999; 267:169–184. [PubMed: 9918669]
- [13]. DiConstanzo L, Moulin M, Haertlein M, Meilleur F, Christianson DW. Arch. Biochem. Biophys. 2007; 465:82–89. [PubMed: 17562323]
- [14]. Cole NB, Murphy DB, Grider T, Reuter S, Brasaemle D, Nussbaum RL. J Biol Chem. 2002; 277:6344–6352. [PubMed: 11744721]
- [15]. Levine RL. Rapid Commun. Mass Spectrom. 2006; 20:1828–1830. [PubMed: 16705654]
- [16]. Apffel A, Fischer S, Goldberg G, Goodley PC, Kuhlmann FE. J. Chromatogr. A. 1995; 712:177–190. [PubMed: 8556150]
- [17]. Dimitrova MN, Peterkofsky A, Ginsburg A. Protein Sci. 2003; 12:2047–2056. [PubMed: 12931002]
- [18]. Ginsburg A, Szczepanowski RH, Ruvinov SB, Nosworthy NJ, Sondej M, Umland TC, Peterkofsky A. Protein Sci. 2000; 9:1085–1094. [PubMed: 10892802]
- [19]. LiCalsi C, Crocenzi TS, Freire E, Roseman S. J. Biol. Chem. 1991; 266:19519–19527. [PubMed: 1655788]
- [20]. Lee BR, Lecchi P, Pannell L, Jaffe H, Peterkofsky A. Arch. Biochem. Biophys. 1994; 312:121–124. [PubMed: 8031118]
- [21]. Hattori H, Crespi HL, Katz JJ. Biochemistry. 1965; 4:1213–1225. [PubMed: 5856627]
- [22]. Kanyo ZF, Scolnick LR, Ash DE, Christianson DW. Nature. 1996; 383:554–557. [PubMed: 8849731]
- [23]. Diez AM, Campo ML, Soler G. Int. J. Biochem. 1992; 24:1925–1932. [PubMed: 1473605]
- [24]. Uversky VN, Eliezer D. Curr. Protein Pept. Sci. 2009; 10:483–499. [PubMed: 19538146]
- [25]. Meilleur F, Contzen J, Myles DA, Jung C. Biochemistry. 2004; 43:8744–8753. [PubMed: 15236583]
- [26]. Ginsburg A, Peterkofsky A. Arch. Biochem. Biophys. 2002; 397:273–278. [PubMed: 11795882]
- [27]. Dimitrova MN, Szczepanowski RH, Ruvinov SB, Peterkofsky A, Ginsburg A. Biochemistry. 2002; 41:906–913. [PubMed: 11790113]
- [28]. Beernink PT, Yang R, Graf R, King DS, Shah SS, Schachman HK. Protein Sci. 2001; 10:528–537. [PubMed: 11344321]
- [29]. Gong S, Blundell TL. PLOS one. 2010; 5:1–12.
- [30]. Yokogaki S, Unno K, Oku N, Okada S. Plant Cell Physiol. 2009; 36:419–423.

- [31]. Savenkova MI, Satterlee JD, Erman JE, Siems WF, Helms GL. *Biochemistry*. 2001; 40:12123–12131. [PubMed: 11580287]
- [32]. Beechem JM, Brand L. *Annu. Rev Biochem*. 1985; 54:43–71. [PubMed: 3896124]
- [33]. Eftink MR. *Methods Biochem Anal*. 1991; 35:127–205. [PubMed: 2002770]
- [34]. Callis PR. *Methods Enzymol*. 1997; 278:113–150. [PubMed: 9170312]
- [35]. Eftink MR, Ghiron CA. *Biochemistry*. 1976; 15:672–680. [PubMed: 1252418]
- [36]. Lakowicz, J. *Principles of Fluorescence Spectroscopy*. Kluwer Academic Publisher; Dordrecht, The Netherlands: 1999.
- [37]. Garrett DS, Seok Y-J, Peterkofsky A, Gronenborn AM, Clore GM. *Nature Struct. Biol*. 1999; 6:166–173. [PubMed: 10048929]
- [38]. Fisher SJ, Helliwell JR. *Acta Crystallographica Section A*. 2008; A64:359–367.
- [39]. Budayova-Spano M, Fisher SZ, Dauvergne MT, gbandje-McKenna M, Silverman DN, Myles DA, McKenna R. *Acta Crystallogr Sect F Struct Biol Cryst Commun*. 2006:9.
- [40]. Liu X, Hanson BL, Langan P, Viola RE. *Acta Crystallogr D Biol Crystallogr*. 2007:1000–1008. [PubMed: 17704569]
- [41]. Luo S, Wehr NB, Levine RL. *Anal. Biochem*. 2006; 350:233–238. [PubMed: 16336940]

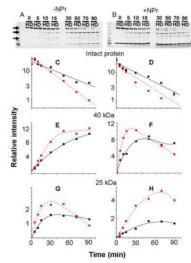


Fig. 2. Limited proteolysis of EI^{Ntr}

Approximately 65 μg of either H-EI^{Ntr}(H356A) or D-EI^{Ntr}(H356A) was incubated with 0.1 μg trypsin in 10 mM Tris-Cl (pH 8), 100 mM NaCl, 2 mM β -mercaptoethanol, 1 mM EDTA and 10 % glycerol in a total volume of 75 μl at room temperature. A companion incubation mixture was supplemented with 56 μg of NPr 1–85. At the indicated times (0 to 90 mins, shown above the lanes), 7.5 μl aliquots were removed and mixed with 7.5 μl of 2 \times Laemmli sample buffer. The samples were run on 4–20% SDS-PAGE gradient gels (Invitrogen), then stained with Coomassie Blue R250 (panels A & B). Lanes labeled H correspond to H-EI^{Ntr} and those labeled D correspond to D-EI^{Ntr}. The stained gels were scanned in an Odyssey near infrared fluorescence scanner (Li-Cor Biosciences) and then the fluorescence of Coomassie Blue [41] was quantitated by the Odyssey software. The intensity of the bands (panels C through H) were measured after subtraction of the background of the gels. Panels C & D, patterns of the degradation of the intact protein, designated by the topmost arrowhead on the left side of panel A; panels E & F, relative amounts of the ~40 kDa peptide (identified as including residues 170–523, mass of 39,794.4, see fig. 2), designated by the center arrowhead; panels G & H, relative amounts of the ~25 kDa peptide (G524-L748, see fig. 2), designated by the lowest arrowhead. Solid lines with squares = H-EI^{Ntr}; dashed lines with circles = D-EI^{Ntr}. Panels A, C, E, and G correspond to proteolysis in the absence of NPr; panels B, D, F and H correspond to proteolysis in the presence of NPr.

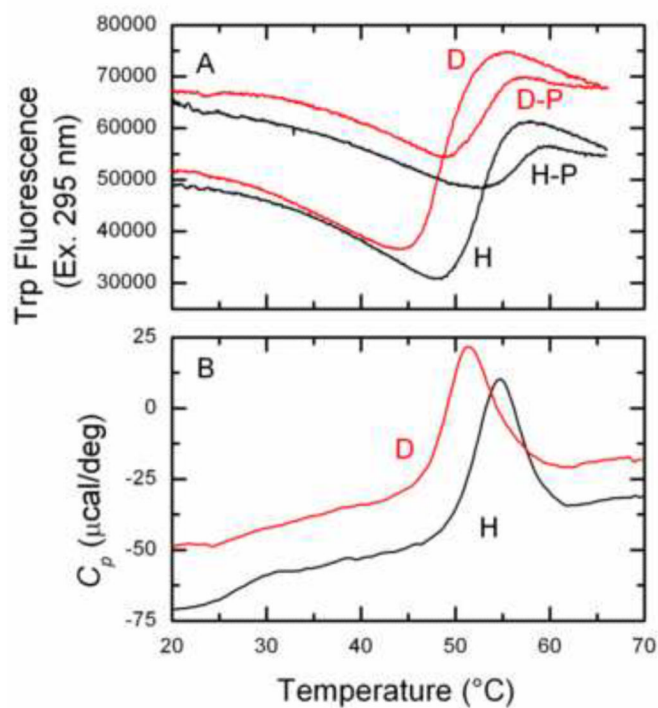


Figure 3. Thermal unfolding of EI^{Ntr}

Panel A: Thermally induced changes in fluorescence. EI^{Ntr}(H356A) in the H and D forms (25 µg/ml) in 20 mM Tris·Cl (pH 8), 2 mM MgCl₂, 5 mM NaCl, 0.1 mM β-mercaptoethanol, 0.05 mM EDTA and 0.5% glycerol in a total volume of 1 ml were scanned through the indicated temperature range at a scan rate of 30 °C/h. Where indicated (H-P and D-P), the samples also contained 150 µM PEP. Excitation was at 295 nm and emission at 340 nm. **Panel B:** DSC scans (see Materials and Methods) of EI^{Ntr}(H356A) H and D forms. The proteins were dialyzed against 10 mM NaPO₄, pH 8 and adjusted to a concentration of 300 µg/ml.

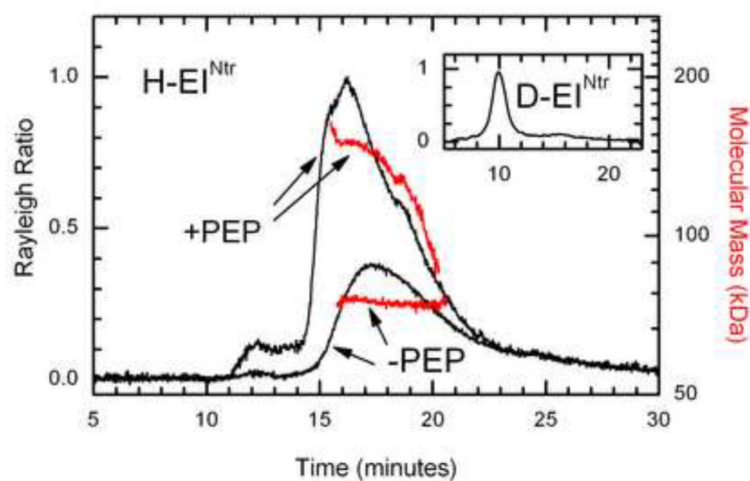


Figure 4. Oligomerization state of EI^{Ntr}

Light scattering analysis of H-EI^{Ntr} was carried out as described in Materials and Methods. The gel filtration column was equilibrated with 20 mM Tris pH 8, 2 mM MgCl₂, 150 mM NaCl. 100 μ l of protein at 0.5 mg/ml was injected. When the protein was run in the presence of PEP, the column was pre-equilibrated with the buffer described above supplemented with 150 μ M PEP. An aliquot (100 μ l of protein at 0.5 mg/ml in the PEP supplemented buffer) was injected onto the column. The masses of the different regions (denoted by the red line) of the eluate were determined. **Inset:** Light scattering analysis of D-EI^{Ntr}. A 100 μ l sample of protein (0.5 mg/ml) was injected onto the column equilibrated with the Tris, MgCl₂, NaCl buffer described above. The horizontal scale is time and the vertical scale is light scattering intensity.

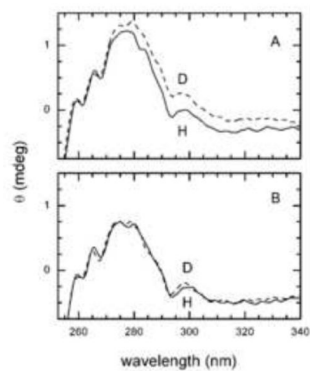


Figure 5. Near UV circular dichroism of EI^{Ntr}

The H and D forms of EI^{Ntr} at 0.6 mg/ml were scanned (16 accumulations) in a Jasco J-715 spectrometer. In panel B, PEP (150 μ M) and MgCl₂ (2 mM) were added.

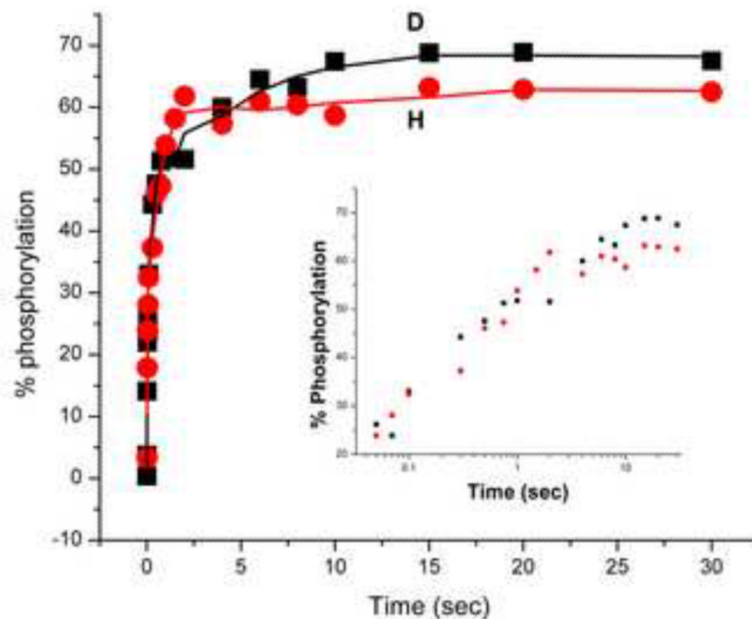


Figure 6. Autophosphorylation of EI^{Ntr}

Preliminary autophosphorylation experiments (with 5 and 10 min incubation periods) were carried out to determine the maximum autophosphorylation of EI^{Ntr} stocks of the dephosphorylated (see Materials and Methods) H and D forms. Kinetic studies were carried out as described in Methods. Filled circles, H-EI^{Ntr}; filled squares, D-EI^{Ntr}. The inset to the figure displays the same data with the time scale plotted logarithmically to clarify the kinetics.

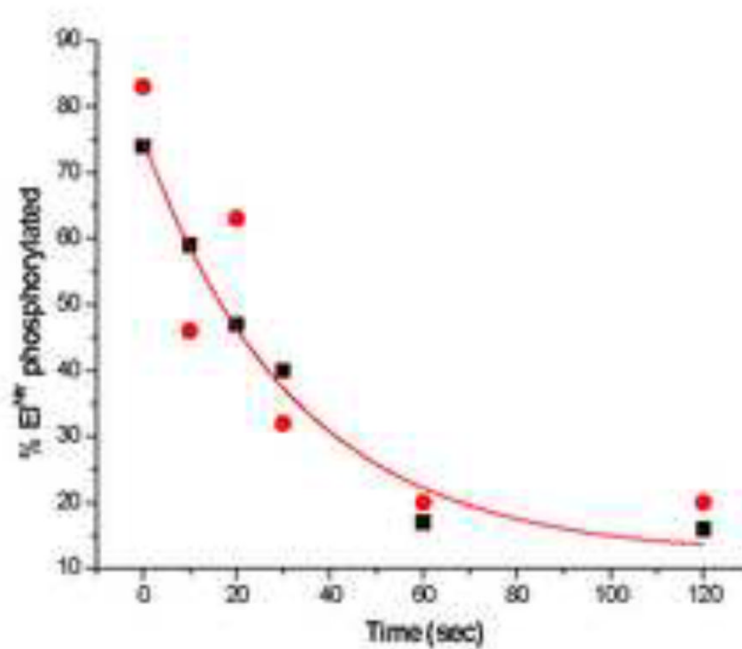


Figure 7. Phosphotransfer from P-EI^{Ntr} to NPr

Kinetics of the phosphotransfer were carried out as described in Methods. Filled circles, D-EI^{Ntr}; filled squares, H-EI^{Ntr}.

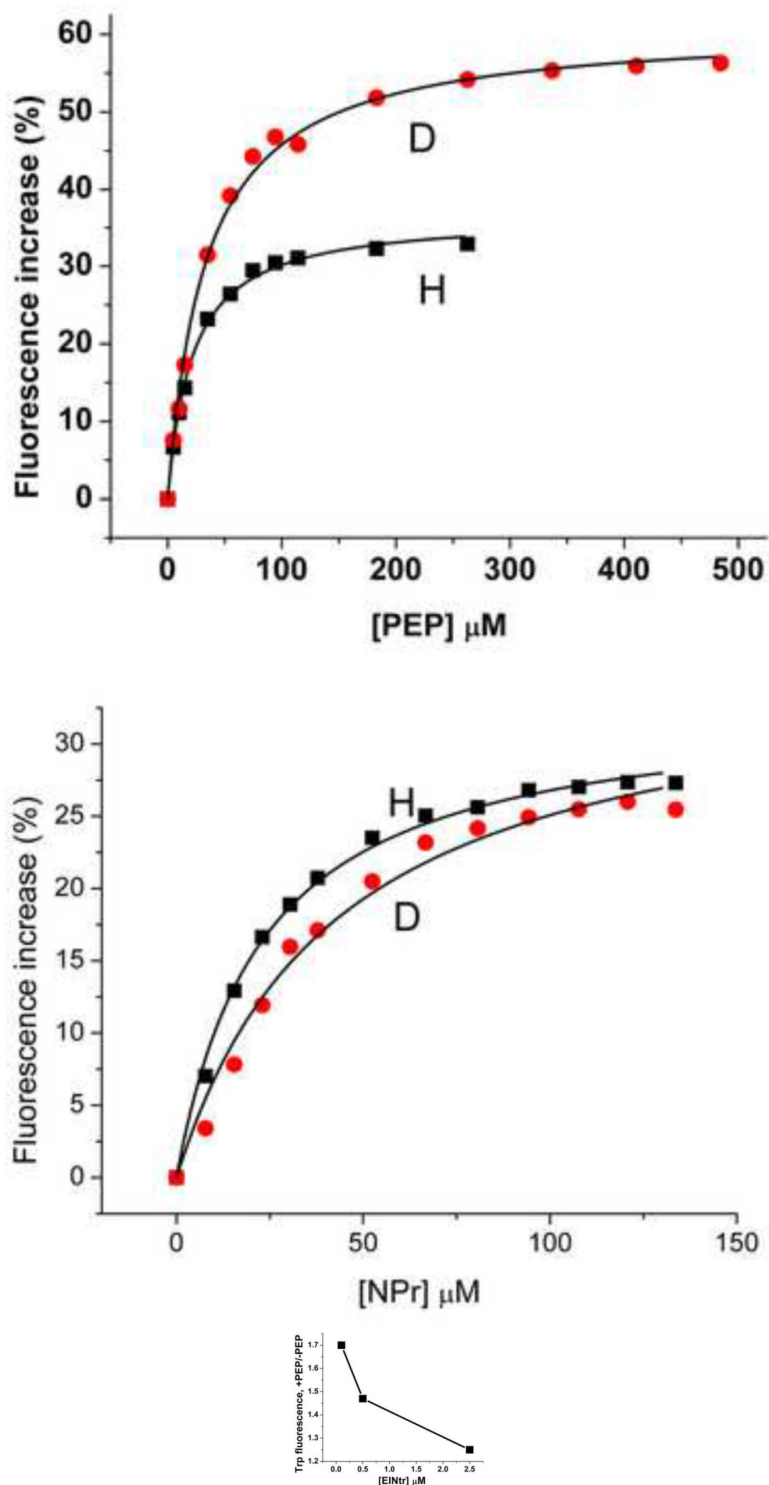


Figure 8. Effect of PEP and NPr concentration on EI^{Ntr} fluorescence

(A) PEP titration: Reaction mixtures (1 ml volume) contained: Tris·Cl, pH 8, 20 mM; MgCl₂, 2 mM, EI^{Ntr}(H356A), 0.5 μM. The baseline fluorescence intensities were: H, 4960; D, 5150. Fluorescence at 340 nm was measured at 37 °C after the indicated additions of

PEP. The increase in fluorescence is plotted against the PEP concentration. An incubation mixture without added EI^{Ntr} showed little fluorescence and no change in fluorescence after addition of PEP (data not shown). H form, squares; D form, circles. The measured fluorescence intensities were expressed as the % increase in fluorescence over the baseline.

(B) NPr titration: Reaction mixtures (1 ml volume) contained: Tris-Cl, pH 8, 20 mM; MgCl₂, 2 mM, EI^{Ntr}(H356A), 0.5 μM. The baseline fluorescence intensities were: H, 5985; D, 4986. Fluorescence at 340 nm was measured at 37 °C after the indicated additions of NPr. The increase in fluorescence is plotted against the NPr concentration. An incubation mixture without added EI^{Ntr} showed some fluorescence change after addition of NPr (data not shown). NPr has no Trp or Tyr residues but does have 3 Phe residues. The sequence is: MTVKQTVEITNKLGMHARPAMKLFELMQGFDAEVLLRNDEGTEAEANSVIALML DSA KGRQIEVEATGPQEEEEALAAVIALFNS. The data were corrected for this change due to the NPr fluorescence. H-EI^{Ntr}, filled squares; D-EI^{Ntr}, open circles. The measured fluorescence intensities were expressed as the % increase in fluorescence over the baseline.

(C) Effect of H-EI^{Ntr} concentration on the PEP-dependent fluorescence change. Experimental conditions were as described above, except that PEP, where added, was at 2 mM. The EI^{Ntr}(H356A) concentration was varied, as indicated.

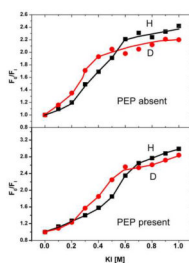


Figure 9. Iodide quench of the fluorescence of EI^{Ntr}

Incubation mixtures (150 μ l total volume) contained Tris·Cl, pH 8, 20 mM; KI and KCl, the sum of which was always 1 M; and EI^{Ntr} (H356A) in the H form (0.98 μ M) or D form (1.36 μ M). Fluorescence was measured with excitation at 295 nm and emission at 340 nm.

Fluorescence quenching was analyzed according to the Stern-Vollmer relationship (F_0/F_1) [35] where F_0 is the fluorescence in the absence of quencher and F_1 is the fluorescence in the presence of the indicated quencher concentration. Filled circles, D- EI^{Ntr} ; filled squares, H- EI^{Ntr} . Upper panel, absence of PEP; lower panel, presence of 2 mM PEP and 2 mM $MgCl_2$.

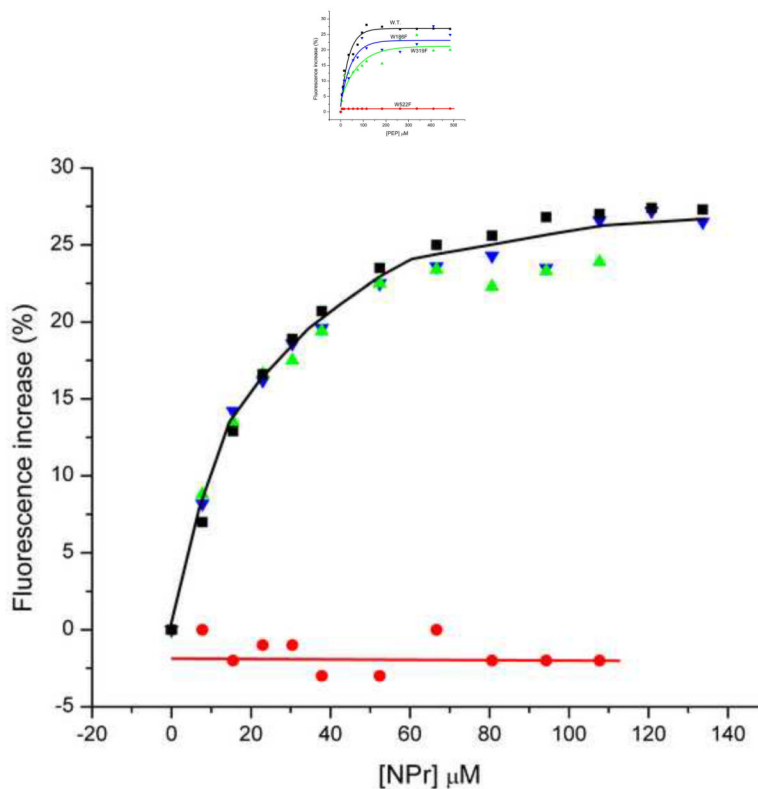


Figure 10. Fluorescence effects on PEP and NPr binding to Trp mutants of EI^{Ntr}

(A) PEP titration: Incubation conditions were as described for Fig. 13, except that the final concentrations of all the EI^{Ntr} proteins used was 82 μg/ml. The baseline fluorescence intensities were: wild-type (filled squares), 42622; W186F (inverted triangles), 41324; W319F (triangles), 37487; W522F (circles), 28078. (B) NPr titration: incubation conditions were as in (A). The baseline fluorescence intensities were: wild-type, 42622; W186F, 72761; W319F, 87741; W522F, 51338.

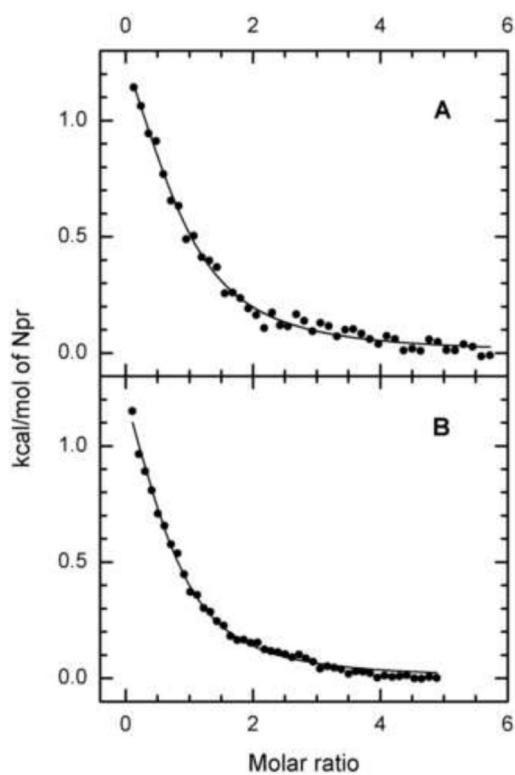


Figure 11. Titration Calorimetry of EI^{Ntr}(H356A) with NPr

Isothermal titration calorimetry was carried out as described in Materials and Methods. Panel A: The concentration of H-EI^{Ntr} was 14 μM and that of NPr in the injection syringe was 380 μM . Panel B: The concentration of D-EI^{Ntr} was 16.4 μM and that of NPr in the injection syringe was 380 μM .

Table IMass Spectrometric Analysis of Deuterated (D) and Hydrogenated (H) EI^{Ntr}

	H	D	% Deuteration ¹
EI^{Ntr} (phospho-form)			
Calculated mass	66,969.8 ²	70,619.8 ³	
Measured mass	66,969.5	70,223.8	89
EI^{Ntr}, Dephosphorylated⁴			
Calculated mass	66,889.8 ⁵	70,609.8 ³	
Measured mass	66,890.7	70,213.6	89
EI^{Ntr} (H356A)			
Calculated mass	66,823.7 ⁵	70,473.7 ³	
Measured mass	66,823.8	70,039.2	88
Active Site Peptide, P₃₅₀₋₃₆₂⁶			
Calculated mass	1,312.5	1,377.5	
Measured mass	1,312.5	1,370.0	88

Mass analysis of the active site peptide and the intact proteins was carried out as described in Methods.

¹The % deuteration is expressed as (Measured mass of D-calculated mass of H/calculated mass of D-calculated mass of H).

²calculated mass corresponds to the protein (mass=66,711.6) which is both phosphorylated (adds 80 mass units) at the active site and gluconoylated [12] (adds 178 mass units) at the site of the His tag sequence.

³The calculated mass of D is expressed as the mass of the protein in which all nonexchangeable hydrogens are replaced by deuterium (perdeuterated protein).

⁴Dephosphorylation was accomplished by treatment with pyruvate and MgCl₂ (see methods).

⁵Calculated mass corresponds to the protein (mass=66,711.6) which is gluconoylated (adds 178 mass units).

⁶Calculated mass corresponds to the protein (mass=66,645.7) which is gluconoylated (adds 178 mass units).

⁷The active site peptide sequence is DGAANSHAAIMVR. The histidine residue is the site of phosphorylation.